

Diffusion of Macromolecules in Dextran Methacrylate Solutions and Gels As Studied by Confocal Scanning Laser Microscopy

S. C. De Smedt,* T. K. L. Meyvis, and J. Demeester

Laboratory of General Biochemistry and Physical Pharmacy, University of Gent, Harelbekestraat 72, 9000 Gent, Belgium

P. Van Oostveldt

Laboratory of Biochemistry and Molecular Cytology, University of Gent, Coupure Links 653, 9000 Gent, Belgium

J. C. G. Blonk

Unilever Research Laboratories Vlaardingen, Olivier van Noortlaan 120, 3133AT Vlaardingen, The Netherlands

W. E. Hennink

Utrecht Institute for Pharmaceutical Sciences, Department of Pharmaceutics, University of Utrecht, 3508 TB Utrecht, The Netherlands

Received January 27, 1997; Revised Manuscript Received May 29, 1997[®]

ABSTRACT: This paper reports the results and the interpretation of rheological experiments on and diffusion measurements of fluorescent polymer chains in solutions and gels of dextran (dex) derivatized with methacrylate (ma) groups. We illustrate the use of confocal scanning laser microscopy (CSLM) and fluorescence recovery after photobleaching (FRAP) to study the mobility of large molecules in polymer systems. The main aim was to understand the influence of the polymer network in the gels on the mobility of large molecules. Therefore we measured the diffusion coefficients before and after cross-linking the dextran methacrylate (dex–ma) chains. Increasing the dex–ma concentration did not spectacularly increase the sterical hindrance by the dex–ma network. However, the sterical hindrance did become significantly stronger when the size of the diffusing probe and the degree of ma substitution were increased. The mobility of the probes decreased when the dex–ma gels became more elastic. However, the decrease in the diffusion coefficient was much less than the spectacular increase in the elasticity of the hydrogels.

Introduction

Although dextran hydrogels are frequently used as column packings in all kinds of chromatographic applications, pharmaceutical research has only recently focused on the potential of dextran hydrogels in the field of controlled drug delivery. Due to the tremendous boom in biotechnology over the past years, a main topic in this field is the stabilization, targeting, and release of therapeutic proteins enclosed in acryldextran microspheres. Moreover, colon drug delivery and nasal drug delivery from dextran hydrogels are under investigation.^{1–5} In these formulations, a key point is to understand how the diffusion process of the drug is influenced by the structure of the polymer network. This fundamental knowledge of probe diffusion in gels would be useful in many other fields such as size exclusion chromatography and gel electrophoresis.

Although there has been considerable progress in the knowledge of the diffusion of probes through polymer networks over the past years, no one has yet been able to come up with a uniform theory, modeling all the influencing parameters. Research still relies upon experimental methods to study the mobility of molecules in polymer matrices. There is a tradition in pharmaceutical research of performing release experiments to study diffusion. However, global release is mostly the result of many complex physicochemical phenomena which occur inside the polymer system. Therefore,

based upon release experiments, it is often difficult to describe the mobility of the probe inside the polymer network. Although diffusion measurements in gels are not a trivial undertaking, several approaches like dynamic light scattering,^{6,7} nuclear magnetic resonance,⁸ and the use of radio labeled probes have been pursued.^{9–13} Interesting reviews on diffusion measurement in gels were published by Muhr and Blanshard¹⁴ and Westrin et al.¹⁵

An important goal of this work was to evaluate the use of confocal scanning laser microscopy (CSLM) for measuring diffusion coefficients (D) in gels. On the basis of the work of Blonk et al.¹⁶ the CSLM was modified to perform FRAP experiments. By the 1970's, FRAP had been introduced by biophysicians to study dynamic phenomena in plasma membranes of cells.^{17,18} Since the 1990's, fluorescence recovery after photobleaching (FRAP) has been used in polymer physics to study the transport of macromolecular tracer molecules in concentrated polymer solutions.^{19–23} FRAP was preferred to dynamic light scattering because the polymers in the matrix scattered too strongly which prevented accurate measurements of the diffusion coefficients of probe molecules in such matrices. Currently, there are only a few papers describing the use of FRAP to determine diffusion coefficients in gels.^{24,25} In comparison to the FRAP instruments used in all the previous studies, the CSLM used in this work refines the FRAP technique. Previous FRAP experiments only provided a fluorescence signal. This new FRAP setup

[®] Abstract published in *Advance ACS Abstracts*, July 15, 1997.

has the advantage of creating digital images of the undestroyed sample. These images can give additional information about the quality of the experiment and the occurrence of flows inside the sample. To our knowledge, only Cutts et al.²⁶ and Wedekind et al.^{27,28} have recently described the use of CSLM for the determination of localized diffusion coefficients in, respectively, agarose gels and glycerol–water mixtures.

This paper evaluates the use of CSLM for the study of the diffusion of fluorescent dextran chains through dextran methacrylate (dex–ma polymer solutions and gels). Therefore we compared probe diffusion in the non-cross-linked dex–ma solutions with that in relaxed and fully swollen dex–ma gels. Data which compare probe diffusion in polymer systems of identical composition before and after cross-linking are rather rare. In this study we tried to identify the influence of the size of the probe on the overall diffusion phenomenon in dex–ma solutions and gels. Another goal of this study was to focus on the relation between the rheological behavior of the dex–ma solutions and gels and the diffusion of probes through these systems. We also investigated the influence of the degree of substitution of the dex–ma and the swelling of the gels on the diffusion of the probes through the gels.

Experimental Section

Dex–ma Preparation and Characterization. The dex–ma batches were prepared and characterized as described in detail elsewhere.^{29,30} The degree of ma substitution (DS, i.e. the number of ma molecules per 100 glucopyranosyl units) was determined by proton nuclear magnetic resonance spectroscopy (¹H-NMR) in D₂O with a Gemini 300 spectrometer (Varian). The DS of the batches used in this study was 5 unless otherwise indicated.

Preparation of the dex–ma Hydrogels. Dex–ma hydrogels were prepared by radical polymerization of aqueous dex–ma solutions (solvent: 0.2 M Na₂HPO₄, 1 mM NaEDTA, pH 8.5) as a function of the dex–ma concentration and the ma substitution. Solution A was obtained by adding 30 μ L of *N,N,N,N'*-tetramethylethylenediamine (TEMED) to a 3.0 mL dex–ma solution, while solution B was a mixture of 2.5 mL of dex–ma solution and 125 μ L of ammonium persulfate (APS; 80 mg/mL). Solution A (2.5 mL) was added to solution B (2.5 mL). Approximately 5 min after solution A was added to solution B (depending on the dex–ma concentration and the DS), gelation started, and it was completely finished after roughly 90 min.³⁰ When those “relaxed” dex–ma gels were immersed into solvent (0.2 M Na₂HPO₄, 1 mM NaEDTA, pH 8.5), their swelling increased. After complete swelling, “swollen” dex–ma gels were obtained.

Fluorescent Probes. The diffusion coefficient measurements were performed with fluorescein isothiocyanate dextran (FITC–dex) probes (Sigma) of several different weight averaged molecular weights (M_w). They were 19 000, 51 000, 148 000, and 487 000 g/mol, containing, respectively, 0.008, 0.004, 0.007, and 0.007 mol of FITC/(mol of glucose). The polydispersity index (M_w/M_n) was less than 1.35. In all of the FRAP experiments the FITC–dex concentration was 0.4 mg/mL as derived from linearity tests (see Results and Discussion).

Diffusion Coefficient Measurements. The diffusion coefficients of FITC–dex probes were measured using the FRAP method.³² In this technique, the translation diffusion coefficient of the fluorescent probe is measured by bleaching the fluorescent molecules moving in the focal area of the laser beam. Immediately after bleaching, a highly attenuated laser beam measures the recovery of the fluorescence in the bleached area due to the diffusion of the fluorescent probe from the surrounding unbleached areas into the bleached area. It is assumed bleaching is an irreversible process. Therefore, fluorescence recovery is considered to be due to diffusion only. The probe diffusion coefficient D can be derived from the

recovery of the fluorescence in the bleached area. The experimental setup of the noncommercial FRAP instrument was based on the pioneering work of Blonk et al.¹⁶ The core of the instrument is a high-resolution confocal scanning laser microscope (MRC-600 Bio-Rad). The instrument is essentially composed of a laser source, a photomultiplier (PMT), and a computer for instrument control and image building. The connected microscope is a Nikon Diaphot 300 used in the inverted mode. The Bio-Rad instrument itself does not allow rapid changes of the laser intensity. However, this is a requirement for the short (30–100 ms) photobleaching times used in this study. Therefore, an additional setup had to be built. It consists of a 1% neutral density filter (5 cm \times 5 cm, Balzers) that is placed in the light path of the laser, before entering the microscope. The filter is fixed on a motor so that it can rotate over 45°. Depending on the position of the filter, either an intense or an attenuated laser beam enters the microscope. The intense beam photobleaches the fluorescent probes which are present in the focal area of the laser. The dex–ma gels were made in FRAP cuvettes of our own design. To make these, the bottom was sawn from a small centrifuge tube. This tube was glued on a cover slide with DPX mountant for histology (Fluka). As diffusion is dependent on temperature, the measurements were performed under temperature control at 25 °C. The FRAP cuvettes fit exactly in the temperature control setup that is driven by a water bath. After introducing the cuvette into the temperature controller, the whole setup is fixed on the stage of the microscope. The sample is allowed to equilibrate for 5 min prior to starting any measurements.

A FRAP experiment consists of a number of steps as described earlier.¹⁶ Summarized, the confocal microscope builds an image by scanning the laser along a plane (xy) in the sample. This plane is the confocal plane, which means that only light emitted from this plane is significantly detected by the PMT. In our experiments, the confocal plane was selected at 50 μ m above the bottom of the FRAP cuvette (Figure 1a). For FRAP measurements, only one line (fixed y) is chosen in the confocal plane (Figure 1b), and the evolution of the fluorescence along this line is followed before and after bleaching. This results in a x – t image (Figure 1d) which enables extraction of the fluorescence recovery curve. Figure 2 illustrates the normalized fluorescence recovery profiles of FITC–dex in a dex–ma solution and a dex–ma gel. The normalized fluorescence recovery curve ($f(t)$) is obtained by dividing the the fluorescence intensities during the recovery by the fluorescence intensity of the bleach spot before bleaching. The diffusion coefficient is calculated from ($f(t)$) as described elsewhere.¹⁶

$$f(t) = \sum_{n=0}^{\infty} \frac{-\kappa^n}{n!} \frac{1}{1 + n[1 + (2t/\tau_D)]} \quad (1)$$

where κ is the bleaching constant. κ is an abstract number that characterizes the “amount” of bleaching. It is influenced by the intensity of the laser beam, the bleach time, and the sensitivity of the fluorescent molecule for bleaching. τ_D is the characteristic diffusion time and is related to the diffusion coefficient by:

$$\tau_D = \omega^2/4D \quad (2)$$

where ω is defined as half the width of the Gaussian intensity profile of the laser spot determined at e^{-2} times the height of the profile. D (cm²/s) is the diffusion coefficient as defined by the Stokes–Einstein equation:

$$D = \frac{kT}{6\pi\eta r_H} \times 10^4 \quad (3)$$

where k is the Boltzmann constant, T is the temperature (K), η is the viscosity (Ns/m²) of the medium, and r_H (m) is the hydrodynamic radius of the diffusing probe.

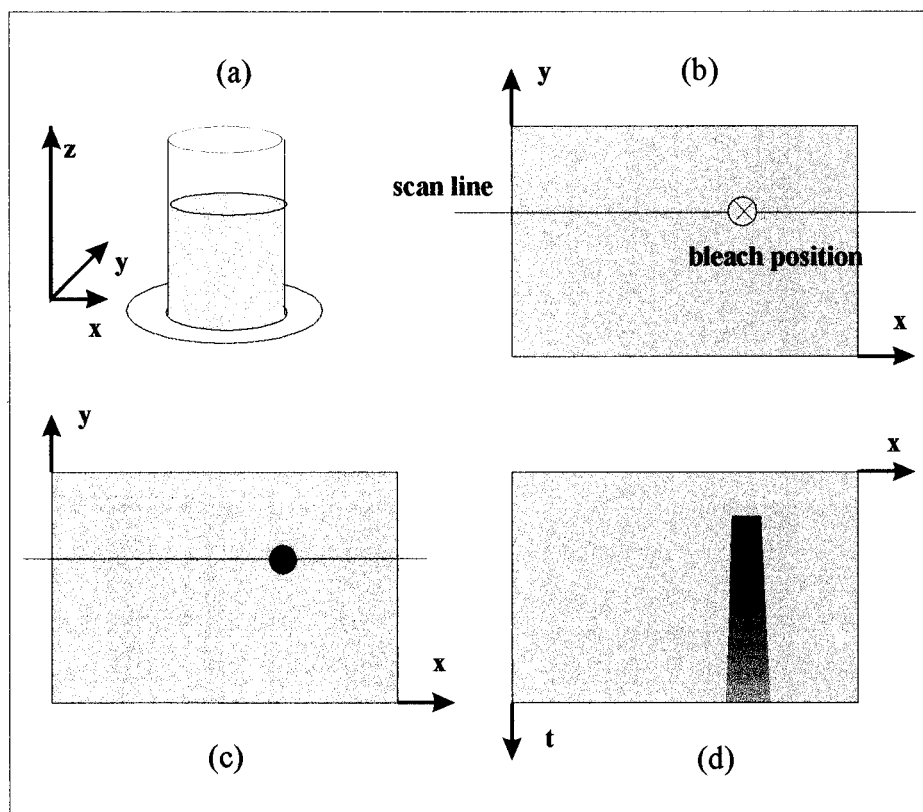


Figure 1. Stepwise illustration of a FRAP experiment. (a) in the sample vial the confocal plane (xy) is set at $50\ \mu\text{m}$ above the bottom (z direction); (b) in the confocal plane a scanning line (y) and a bleach position (x) on this line are chosen; (c) the laser is parked at the bleach position and the spot is bleached; (d) the recovery image ($x-t$) is constructed. For more detail, see text; the proportions are not respected in this figure.

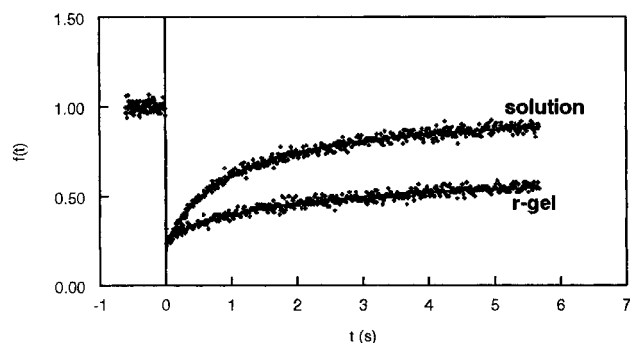


Figure 2. Fluorescence recovery curves of FITC-dex 487 000 in a dex-ma solution and a relaxed dex-ma hydrogel (r-gel). The dex-ma concentration was $100\ \text{mg/mL}$ in both the solution and the gel.

Due to chemical interactions between fluorescent probes and the polymer network a fraction of the fluorescent probes might be immobile. This would result in a partial fluorescence recovery after bleaching. The following fluorescence recovery equation takes the presence of immobile fluorescent probes into account:

$$F(t) = F(i)[1 - R(1 - f(t))] \quad (4)$$

where $F(i)$ is the fluorescence intensity of the bleach spot before bleaching and R is the mobile fraction defined as:

$$R = \frac{F(\infty) - F(0)}{F(i) - F(0)} \quad (5)$$

where $F(\infty)$ is the normalized fluorescence intensity of the bleached spot at infinite time after bleaching and $F(0)$ is the normalized fluorescence intensity of the bleach spot just after bleaching (see Figure 2).

Rheological Measurements. Viscosity measurements on the saccharose solutions were performed at $25 \pm 0.1\ ^\circ\text{C}$ with a calibrated capillary viscosimeter (Lauda equipped with Ubbelohde capillaries). The dynamic viscosity was calculated from the kinematic viscosity by means of reported density values.³⁴ The dynamic viscosity of the dex-ma solutions and the elasticity of the relaxed dex-ma gels were measured at $25 \pm 0.1\ ^\circ\text{C}$ by means of a CSL2 500 controlled stress rheometer from TA-Instruments. Creep experiments were carried out to optimize the applied stress and to check for slip effects in frequency-oscillation measurements which were performed to measure the elasticity of the dex-ma gels. The details of the experimental procedure are described elsewhere.³⁰

Release Experiments. Release experiments were performed on dex-ma hydrogels loaded with bovine albumin (BA, Sigma) or fluorescein isothiocyanate bovine albumin (FITC-BA, Sigma). The FITC content of FITC-BA was $11.2\ \text{mol}$ of FITC/(mol of BA). The proteins, dissolved in phosphate buffer, were added to the native dex-ma solutions. After being stirred for 5 min, the gelation reagents were added as described earlier. To prepare small cylindrical gels, $2\ \text{mL}$ of this gelling solution was transferred to a syringe ($5\ \text{mL}$) and left to gel for 90 min. The total protein content of each gel was $3\ \text{mg}$. In addition nonprotein loaded gels were made as a reference. Release experiments were done by submerging the protein loaded cylindrical gel into phosphate buffer ($45\ \text{mL}$) at room temperature. The protein content in the buffer samples was measured by means of the BIORAD protein assay, using the microassay procedure.³³ The absorption was measured on a Biochrom spectrophotometer (Pharmacia) using the buffer in which the nonloaded gels were submerged as a reference.

Swelling Experiments. To characterize the swelling behavior of the dex-ma hydrogels, the volumes of the hydrogels in the relaxed and in the swollen state were measured. The swelling measurements were performed gravimetrically on the cylindrical dex-ma hydrogels, as described elsewhere.³⁰ The volume of the hydrogels was determined using the

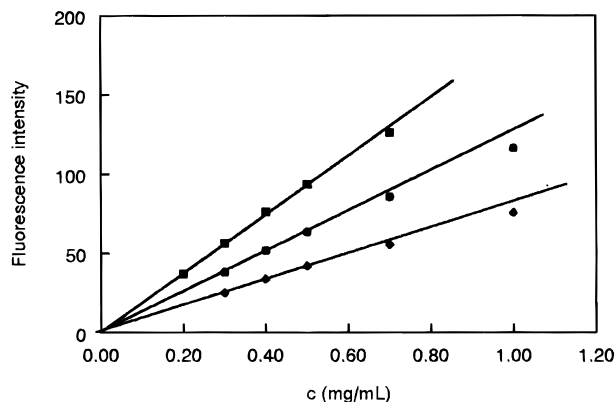


Figure 3. Fluorescence intensity as a function of the FITC-dex concentration (MW 148 000). The fluorescence was measured at different gain settings of the PMT: 750 (■), 700 (●), and 650 (◆). The standard deviation is not indicated when it is smaller than the size of the marker.

buoyancy principle of Archimedes:

$$V_{g,r} = \frac{W_{a,r} - W_{h,r}}{\rho_h} \quad (6)$$

$$V_{g,s} = \frac{W_{a,s} - W_{h,s}}{\rho_h} \quad (7)$$

In eqs 6 and 7 $V_{g,r}$ and $V_{g,s}$ are respectively the volume of the hydrogel in the relaxed and the swollen state, while $W_{a,r}$ and $W_{h,r}$ are respectively the weight of the hydrogel in air and in hexane (being a nonsolvent for the dex-ma hydrogels). ρ_h is the density of hexane at the experimental temperature (0.659 g/mL at 20 °C).

Results and Discussion

Evaluation of the Probe Concentration. Before FRAP experiments were performed on dex-ma gels, it was necessary to determine the appropriate FITC-dex concentration range. If the FITC-dex concentration is too high, the PMT saturates. This results in a fluorescence registration that is lower than the actual fluorescence emitted by the probes. Moreover, high FITC-dex concentrations increase the probability that fluorescence light emitted by one molecule is absorbed by a neighboring molecule. This phenomenon, which is known as the "inner filter effect",³⁵ also decreases the signal at the PMT. As FRAP is based on the dynamics of a quantitative fluorescence change, measurements have to be done on samples with appropriate probe concentrations. Figure 3 illustrates a nonlinearity when the FITC-dex concentration becomes too high. The FITC-dex concentration used in all of the FRAP experiments (0.4 mg/mL) is in the linear concentration region. Moreover, the fluorescence intensity calculated after extrapolation of the FITC-dex concentration to zero does not differ significantly from zero. This indicates a correct blank setting of the PMT.

Evaluation of the Diffusion Coefficients As Measured by FRAP. To determine if the instrument is operating properly, the diffusion coefficient of FITC-dex chains with different molecular weights (MW) was measured in saccharose solutions. The Stokes-Einstein equation (eq 3) describes the diffusion of strongly diluted spherical molecules in a pure viscous medium. It indicates a linear relationship between D and $1/\eta$. Figure 4 shows that the diffusion coefficient of the FITC-dex chains varies linearly as a function of the reciprocal value of the viscosity of the saccharose

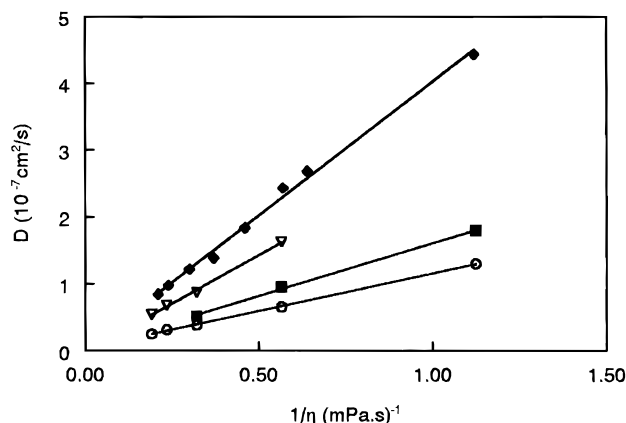


Figure 4. Diffusion of FITC-dex as a function of the reciprocal dynamic viscosity of the saccharose solutions and the molecular weight of FITC-dex: 19 000 (◆), 51 000 (▽), 148 000 (■), and 487 000 (○). The standard deviation is not indicated when it is smaller than the size of the marker.

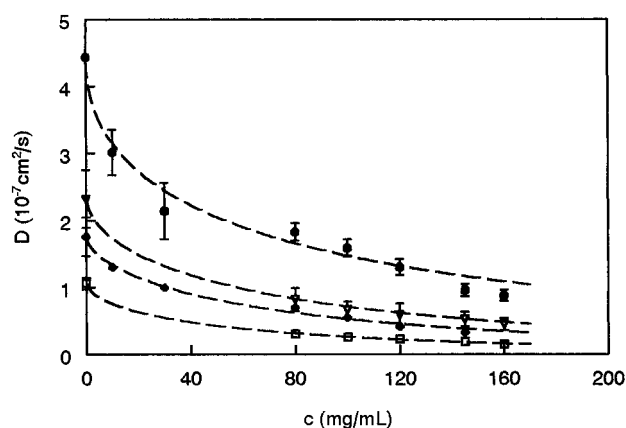


Figure 5. Diffusion of FITC-dex in dex-ma solutions as a function of the dex-ma concentration and the molecular weight of FITC-dex: 19 000 (◆), 51 000 (▽), 148 000 (■), and 487 000 (○). The standard deviation is not indicated when it is smaller than the size of the marker.

solutions. Moreover, the diffusion coefficient calculated after extrapolation to $1/\eta = 0$ does not differ significantly from zero, as expected by the Stokes-Einstein equation. The different slopes in Figure 4 also show the influence of the hydrodynamic size of FITC-dex chains on the diffusion.

Study of the Diffusion of FITC-dex Chains in dex-ma Solutions. The diffusion coefficient of FITC-dex chains was measured in dex-ma solutions ($D_{sol.}$) as a function of the dex-ma concentration. Figure 5 shows the results. Each point in the graph is an average of 15 FRAP measurements. It is clear that the FITC-dex chains diffuse more slowly when the dex-ma concentration is increased. The diffusion in polymer solutions ($D_{sol.}$) is often described by the equation suggested by Phillies et al.:³⁶

$$D_{sol.} = D_0 e^{-ac^v} \quad (8)$$

where D_0 is the diffusion coefficient in the solvent, c is the concentration of the polymer solution, and a and v are parameters determined by the polymer concentration and the size of the probe, which were interpreted by the authors in a previous study. Although more experimental points could be recommended, we did fit the data represented in Figure 5 to eq 8. In the fitting procedure (nonweighted nonlinear least squares method),

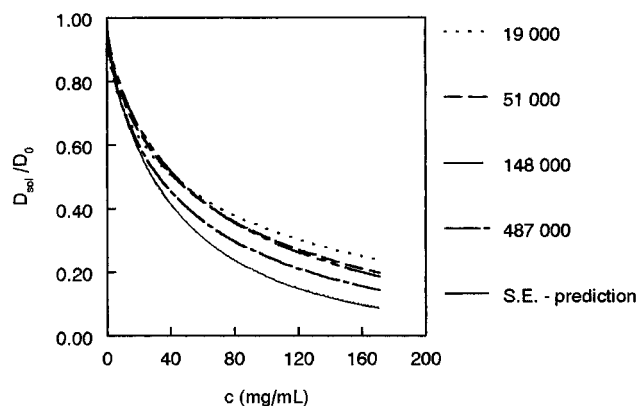


Figure 6. Relative diffusion coefficient as a function of the concentration of the dex-ma solutions for FITC-dex of different molecular weight. The profile of D_{sol}/D_0 as predicted by the Stokes-Einstein (S.E.) equation (eq 3) was calculated from the dynamic viscosity of the dex-ma solutions.

three parameters were simultaneously fitted: D_0 , a , and v . As there was also an experimental error on D_0 , we preferred to consider it as a free parameter in the fitting procedure. Figure 5 shows the data points are well fitted to eq 8. This was confirmed by the random scattering of experimental points around the fitted curves. Figure 6 shows the relative diffusion coefficient (D_{sol}/D_0) of the FITC-dex chains as a function of the dex-ma concentration. The curves are based on the regression lines from Figure 5. Figure 6 shows the probe diffusion in the dex-ma solutions did not go as expected by the Stokes-Einstein equation (eq 3), which predicts the diffusion coefficient to be in inverse proportion to the macroscopic dynamic viscosity of the dex-ma solutions. In all of the experiments, especially at higher dex-ma concentrations, the probe molecules moved more quickly through the dex-ma solutions than predicted by the Stokes-Einstein equation. Deviations from the Stokes-Einstein equation decreased as the size of the FITC-dex chains was increased: the dex-ma solutions retarded large FITC-dex chains stronger than small ones. This agrees with previously reported results on the diffusion of FITC-dex chains in non-derivatized dextran solutions.³⁷ The concentration dependence of the dynamic viscosity of the dex-ma solutions (data not shown) indicated that most of the dex-ma solutions belonged to the transition region between dilute and semidilute solutions. Some of them were semidilute solutions. This means that the dex-ma concentration in the solution is higher than the critical concentration at which the polymer chains start to entangle.³⁸ This deviation of the diffusion profiles in semidilute polymer solutions from the profile predicted by the Stokes-Einstein equation was investigated in detail by Phillies et al.³⁶

Study of the Diffusion of FITC-dex Chains in Relaxed dex-ma Gels. The diffusion coefficient of FITC-dex chains was measured in relaxed dex-ma gels (D_{r-gel}). Figure 2 shows the fluorescence recovery curves of FITC-dex chains in dex-ma solutions and gels. The experimental points in Figure 2 were fit to eq 1. While a complete fluorescence recovery (for $t \rightarrow \infty$) was observed in dex-ma solutions, the fluorescence recovered only partially in the relaxed dex-ma gels. Figure 7 shows the percent of fluorescence recovery as a function of the dex-ma concentration and the DS of dex-ma. The percent of fluorescence recovery decreased as the dex-ma concentration and the DS increased. A partial fluorescence recovery indicates

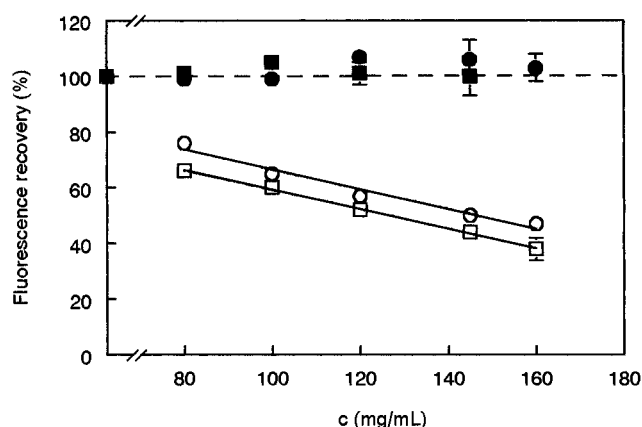


Figure 7. Percent of fluorescence recovery in dex-ma solutions (closed symbols) and dex-ma gels (open symbols) as a function of the dex-ma concentration and the degree of ma substitution: DS 5 (\square , \blacksquare) and DS 3 (\circ , \bullet). The probe was FITC-dex 487 000.

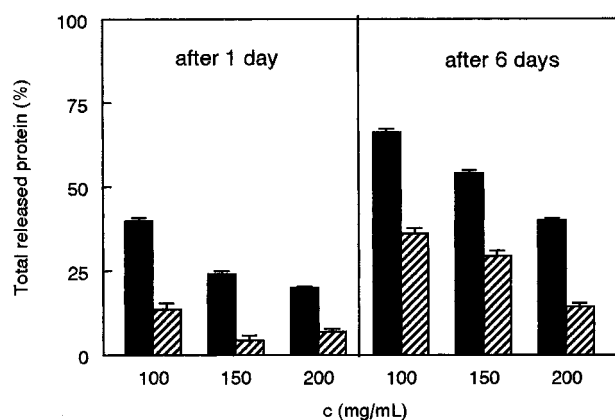


Figure 8. Total amount of protein released after 1 and after 6 days from dex-ma gels with different dex-ma (DS 7.5) concentrations: FITC-BA (striped bars) and BA (black bars).

immobile fluorescent molecules.³² Although no real proof exists, an explanation for the partial fluorescence recovery in the dex-ma gels could be a hydrophobic adsorption of FITC molecules, present on the dextran chains, to the ma groups of the dex-ma network. If hydrophobic adsorption exists in the dex-ma gels, it can also be expected to occur in dex-ma solutions. However, unlike the intermolecular complexes in dex-ma gels, those formed in dex-ma solutions remain mobile so that a complete fluorescence recovery remains possible. Consequently, we have to take into account that both free FITC-dex chains and FITC-dex/dex-ma intermolecular complexes could contribute to the fluorescence recovery in dex-ma solutions.

Another plausible explanation for the immobilization could be a steric blockage of the diffusion of FITC-dex chains due to the presence of very small meshes in the dex-ma gels. It can be assumed that only a minor difference in size exists between a FITC labeled macromolecule and its unlabeled equivalent. Therefore, if this "sterical entrapment explanation" were correct, it could be expected that the macroscopically observed release of labeled and unlabeled macromolecules from dex-ma gels would be equivalent. Release experiments were performed to challenge this presumption. Instead of dextran, bovine albumin and fluorescent labeled bovine albumin were used since they are easier to detect by means of the same assay. Figure 8 clearly shows for all the dex-ma gels that the percentage of FITC-BA released after 6 days is lower than the percentage of

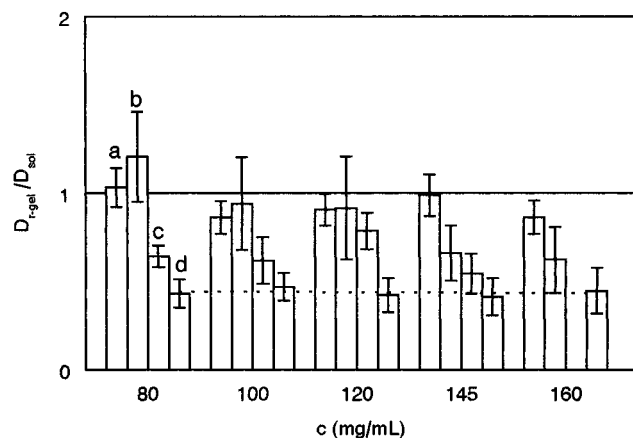


Figure 9. Ratio of the diffusion coefficient in dex-ma gels to the diffusion coefficient in dex-ma solutions as a function of the dex-ma concentration and the molecular weight of FITC-dex: (a) 19 000, (b) 51 000, (c) 148 000, and (d) 487 000. The dotted trend line illustrates the ratio of the diffusion coefficients for FITC-dex 487 000 does not change significantly when the dex-ma is increased.

BA released over the same period. This observation suggests that the partial fluorescence recovery is explained by adsorption of FITC-dex chains rather than by the sterical blockade hypothesis. As we were especially interested in the sterical hindrance of the dex-ma network on the diffusion of macromolecular probes, the indication for adsorption between FITC-dex chains and dex-ma chains made it more difficult to unravel this sterical hindrance. However, the partial fluorescence recovery revealed unexpected physicochemical phenomena which might be pharmaceutically useful for the release of hydrophobic drugs from dex-ma gels. A more profound study will try to unravel this effect.

Although there is only a partial fluorescence recovery in the dex-ma gels, Figure 2 clearly shows that there are still mobile FITC-dex chains which do diffuse through the dex-ma network. In further explanation of our results, we assumed if adsorption did exist, the adsorbed FITC-dex chains would not interfere with the diffusion of those free FITC-dex chains. Furthermore, we assumed the junctions in the dex-ma gels introduced by the gelation would not introduce new chemical interactions with the FITC-dex chains. Therefore, the comparison between D_{r-gel} and $D_{sol.}$ enabled us to investigate specifically the sterical hindrance of the dex-ma network on the diffusion of the free FITC-dex chains. Figure 9 shows, over the whole concentration range, the dex-ma networks themselves do not retard sterically the diffusion of the smallest FITC-dex chain ($D_{r-gel} \approx D_{sol.}$). The hydrodynamic diameter (d_H) of FITC-dex 19 000 is about 6 nm. The second smallest FITC-dex chain is only hindered at higher dex-ma concentrations (MW 51 000, $d_H \approx 10$ nm), while the FITC-dex chain with MW 148 000 ($d_H \approx 16$ nm) is retarded ($D_{r-gel} < D_{sol.}$) over the whole concentration range. The largest one (MW 487 000, $d_H \approx 32$ nm) is retarded even stronger ($D_{r-gel} \ll D_{sol.}$). The hydrodynamic diameters were estimated from the diffusion coefficients measured in saccharose solution using eq 3. Figure 9 shows that increasing the size of the diffusing tracer molecules induces a stronger retardation by the network than increasing the polymer concentration of the hydrogel. Our results agree with the results of Rotstein et al.⁶ and Pajevic et al.⁷ who compared the diffusion of linear polystyrene chains (with different MW) in poly(vinyl methyl ether) solu-

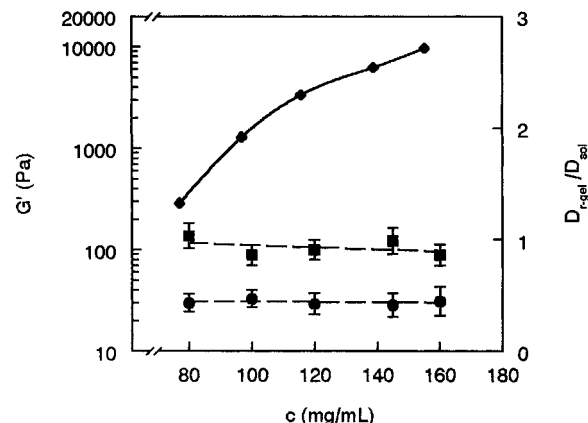


Figure 10. Elasticity modulus (\blacklozenge) and the ratio of the diffusion coefficient in dex-ma gels to the diffusion coefficient in dex-ma solutions as a function of the dex-ma concentration for two different probes: FITC-dex 19 000 (\blacksquare) and FITC-dex 487 000 (\bullet).

tions and gels. The diffusivity in the gels was always less than or equal to the diffusivity in the solutions. Our results support the observation that chemical cross-linking of a polymer solution does not necessarily influence the translation diffusion coefficient of probes. Johansson et al.⁹⁻¹¹ also showed that the chemical cross-linking of κ -carrageenan solutions did not alter the diffusion of poly(ethylene glycol) chains with a molecular weight between 300 and 4000.

Another aim of this study was to clarify the relation between the rheological behavior of the dex-ma solutions and gels and the diffusion of probes through these systems. As explained earlier, Figure 5 shows the macroscopic dynamic viscosity of the dex-ma solutions cannot be taken as a measurement for the diffusion of the FITC-dex chains through the dex-ma solutions. Figure 10 shows the elasticity of the relaxed dex-ma gels and $D_{r-gel}/D_{sol.}$ of FITC-dex chains as a function of the dex-ma concentration. The elasticity of a gel is directly related to its cross-link density. Although an increase in dex-ma concentration results in important changes of the rheological behavior (elasticity) of the gels, the effect on sterical hindrance of the FITC-dex chains is limited. A higher cross-link density can, however, be expected to result in smaller mesh sizes within the network. The unknown functionality of the junctions and the presence of intramolecular cross-links in dex-ma gels did not allow us to use mathematical models which would allow one to calculate the extent of these changes.³⁰ However, the data illustrate that the elasticity of gels cannot be used to predict changes in the diffusivities of FITC-dex chains through the network.

Influence of the Degree of Substitution of dex-ma on the Diffusion of FITC-dex Chains. While the DS hardly influences the diffusion of FITC-dex chains in the dex-ma solution, it does influence the diffusion of FITC-dex chains in the dex-ma hydrogels (data not shown). Roughly speaking, the diffusion in dex-ma gels prepared with the lower substituted dex-ma appears to be 30% faster. As explained in detail previously, a change in the DS will influence the network structure of the gel.³⁰ Not only the total number of cross-links in the gel but also the ratio between inter- and intramolecular cross-links depends on the DS. These phenomena all influence the network architecture and might be responsible for the changes in the diffusion coefficients. However, on the basis of

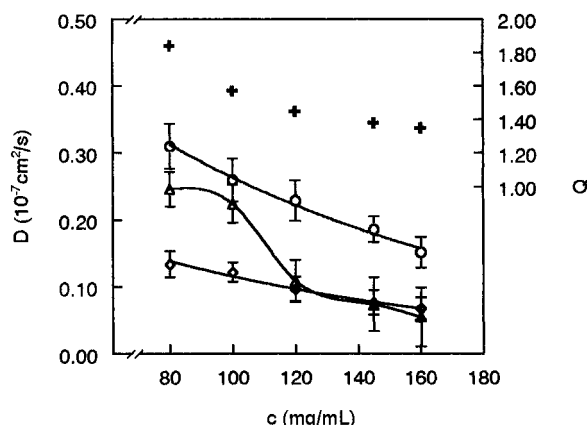


Figure 11. Diffusion coefficient of FITC-dex 487 000 in dex-ma solutions (○), relaxed dex-ma gels (◇), and swollen dex-ma gels (△) as a function of the dex-ma concentration. The swelling capacity Q (+) of the dex-ma gels is also represented. The standard deviations on Q were smaller than the size of the marker.

the dex-ma network characterization as described in a previous publication³⁰ and the diffusion information as described in this paper, it is not yet possible to evaluate if the intermolecular junctions retard the diffusion of macromolecular probes differently from intramolecular junctions.

Study of the Diffusion of FITC-dex-ma Chains in Swollen dex-ma Gels. This study mainly focused on probe diffusion in dex-ma solutions and relaxed gels. However, it was interesting to evaluate if the FRAP setup would allow us to detect the influence of swelling of the dex-ma gels on the diffusion coefficient of the FITC-dex chains. Therefore, solvent was added to the cuvettes on top of the gels. The gels were left to swell for at least 1 week at 25 °C. The swelling capacity (Q) was defined as the ratio of $V_{g,r}$ and $V_{g,s}$ (see eqs 6 and 7). Figure 11 shows the results. For low concentrated swollen gels, FRAP did measure an increase of the diffusion coefficient. For strongly concentrated gels, although significant swelling was observed, no significant difference in the diffusion coefficients was measured. A minimal swelling seems necessary in order to significantly enhance the mobility of large molecules inside the gels, as studied in this paper. The influence of swelling of the dex-ma gels on the diffusion of macromolecular probes might be explained by two phenomena. Analogous to dex-ma solutions (Figure 5), a decrease of the dex-ma concentration in the gels might increase the D of the FITC-dex chains in swollen gels. Moreover, due to swelling, the dex-ma chains between the junctions of the dex-ma network might expand. Consequently, the mesh size of the network gets larger which might weaken the steric hindrance of the dex-ma network on the diffusion of the FITC-dex chains.

Summary

This paper reports the results and the interpretation of probe diffusion measurements in dex-ma solutions and gels as a function of the molecular weight of the probe, the dex-ma concentration, and the degree of ma substitution. Diffusion measurements were performed by means of confocal laser scanning microscopy. It was shown that FITC-dex chains diffuse more slowly in dex-ma solutions as the dex-ma concentration is increased. However, especially at higher dex-ma concentrations the FITC-dex chains move more quickly

through the solutions than can be predicted on the basis of the macroscopic dynamic viscosity of the dex-ma solutions. Failures of the Stokes-Einstein equation decreased as the size of the FITC-dex chains was increased. The partial fluorescence recovery in the dex-ma gels and the release experiments performed with the dex-ma gels indicate that chemical interactions between the FITC-dex chains and the dex-ma might be present. One aim of the paper was to understand the steric hindrance of the dex-ma network on the probe diffusion. Assuming the adsorbed FITC-dex chains do not interfere with the diffusion of the free FITC-dex chains, we illustrated the steric influence of the dex-ma network on the diffusion of the FITC-dex chains. While the dex-ma network did not sterically retard the diffusion of the small FITC-dex chains, it did retard the diffusion of the largest ones. These results suggested that the ratio of the molecular size of the diffusing FITC-dex chains to the mesh size of the dex-ma network plays an important part in the diffusion of macromolecules through the dex-ma gels. Another aim of the study was to clarify the relation between the macromolecular probe diffusion through the dex-ma gels and the rheological properties of the gels. The diffusion in the dex-ma gels slowed down when their elasticity was increased. However, the decrease in the diffusion coefficient was much slighter than the increase in the elasticity of the hydrogels. Especially for the largest FITC-dex chains the steric hindrance of the network on the diffusion did not become significantly stronger when the dex-ma concentration of the hydrogels was increased. However, the steric hindrance by the dex-ma network did become significantly stronger when the size of the diffusing probe was increased. From a pharmaceutical point of view it was interesting to note that adsorption to the dex-ma network might influence the release of hydrophobic drugs from the dex-ma gels. Additionally, if a strong steric hindrance by the dex-ma network were to be pharmaceutically required, it would seem more efficient to increase the size of the diffusing tracer molecules than to increase the dex-ma concentration of the hydrogel.

Acknowledgment. S.C.De S. is a postdoctoral fellow of FWO-Vlaanderen. T.K.L.M. is a doctoral fellow of IWT. The financial support of both institutes is acknowledged with gratitude.

References and Notes

- (1) Edman, P.; Ekman, B.; Sjöholm, I. *J. Pharm. Sci.* **1980**, *69*, 838.
- (2) Hennink, W. E.; Talsma, H.; Borchert, J. C. H.; De Smedt, S. C.; Demeester, J. *J. Controlled Release* **1995**, *39*, 47.
- (3) Brondsted, H.; Hovgaard, L.; Simonsen, L. *Eur. J. Pharm. Biopharm.* **1995**, *6*, 341.
- (4) Simonsen, L.; Hovgaard, L.; Mortensen, P. B.; Brondsted, H. *Eur. J. Pharm. Biopharm.* **1995**, *6*, 329.
- (5) Pereswetoff-Morath, L.; Edman, P. *Int. J. Pharm.* **1996**, *128*, 23.
- (6) Rotstein, N. A.; Lodge, T. P. *Macromolecules* **1992**, *25*, 1316.
- (7) Pajevic, S.; Bansil, R.; Konak, C. *Macromolecules* **1993**, *26*, 305.
- (8) Altenberger, A. R.; Tirrel, M. *J. Chem. Phys.* **1984**, *80*, 2208.
- (9) Johansson, L.; Löfroth, J. E. *J. Colloid Interface Sci.* **1991**, *142*, 116.
- (10) Johansson, L.; Skantze, U.; Löfroth, J. E. *Macromolecules* **1991**, *24*, 6019.
- (11) Johansson, L.; Elvingson, C.; Löfroth, J. E. *Macromolecules* **1991**, *24*, 6024.
- (12) Johansson, L.; Löfroth, J. E. *J. Chem. Phys.* **1993**, *98*, 7471.

- (13) Johansson, L.; Hedberg, P.; Löfroth, J. E. *J. Chem. Phys.* **1993**, *97*, 747.
- (14) Muhr, A. H.; Blanshard, J. M. V. *Polymer* **1982**, *23*.
- (15) Westrin, B. A.; Axelsson, A.; Zacchi, G. *J. Controlled Release* **1994**, *30*, 189.
- (16) Blonk, J. C. G.; Don, A.; Van Aalst, H.; Birmingham, J. J. *J. Microsc.* **1993**, *169*, 363.
- (17) Berk, D. A.; Yuan, F.; Leunig, M.; Jain, R. K. *Biophys. J.* **1993**, *65*, 2428.
- (18) Shargel, L.; Yu, A. B. C. *Applied Biopharmaceutics and Pharmacokinetics*, 3rd ed.; Prentice-Hall International Ltd.: London, 1996.
- (19) Bu, Z.; Russo, P. S. *Macromolecules* **1994**, *27*, 1187.
- (20) Kaufman, E. N.; Jain, R. K. *Biophys. J.* **1994**, *60*, 596.
- (21) Tinland, B.; Borsali, R. *Macromolecules* **1994**, *27*, 2141.
- (22) Wattenbarger, M. R.; Bloomfield, V. A.; Bu, Z.; Russo, P. S. *Macromolecules* **1992**, *25*, 5263.
- (23) De Smedt, S. C.; Lauwers, A.; Demeester, J.; Engelborghs, Y.; De Mey, G.; Du, M. *Macromolecules* **1994**, *27*, 141.
- (24) Moussaoui, M.; Benlyas, M.; Wahl, P. *J. Chromatogr.* **1991**, *558*, 71.
- (25) Moussaoui, M.; Benlyas, M.; Wahl, P. *J. Chromatogr.* **1995**, *591*, 115.
- (26) Cutts, L. S.; Roberts, P. A.; Adler, J.; Davies, M. C.; Melia, C. D. *J. Microsc.* **1995**, *180*, 131.
- (27) Wedekind, P.; Kubitscheck, U.; Heinrich, O.; Peters, R. *Biophys. J.* **1996**, *71*, 1621.
- (28) Wedekind, P.; Kubitscheck, U.; Peters, R. *J. Microsc.* **1994**, *176*, 23.
- (29) Van Dijk-Wolthuis, W. N. E.; Franssen, O.; Talsma, H.; Van Steenberghe, M. J.; Kettenes-Van Den Bosch, J. J.; Hennink, W. E. *Macromolecules* **1995**, *28*, 6317.
- (30) De Smedt, S. C.; Lauwers, A.; Demeester, J.; Van Steenberghe, M. J.; Hennink, W. E.; Roefs, S. P. F. M. *Macromolecules* **1995**, *28*, 5082.
- (31) Van Dijk-Wolthuis, W. N. E.; Kettenes-van den Bosch, J. J.; van der Kerk-van Hoof, A.; Hennink, W. E. *Macromolecules*, in press.
- (32) Axelrod, D.; Koppel, D. E.; Chlessinger, J.; Elson, E.; Webb, W. W. *Biophys. J.* **1976**, *16*, 1055.
- (33) Bradfort, M. M. *Anal. Biochem.* **1976**, *72*, 248.
- (34) Weast, R. C. *Handbook of Chemistry and Physics*, 52nd ed.; The Chemical Rubber Co.: Cleveland, OH, 1971.
- (35) Van Oostveldt, P.; Bauwens, S. *J. Microsc.* **1990**, *158*, 121.
- (36) Phillies, G. D. J.; Ullmann, G. S.; Ullman, K.; Lin, T. H. *J. Chem. Phys.* **1985**, *82*, 5242.
- (37) Furakawa, R.; Arauz-Lara, J. L.; Ware, B. R. *Macromolecules* **1991**, *24*, 599.
- (38) Fujita, H. *Polymer solutions*; Elsevier Science Publishers: Amsterdam, 1990.

MA970100Y